J Therm Anal Calorim (2012) 110:823–829
DOI 10.1007/s10973-011-1972-0

Non-isothermal kinetic analysis on the crystallization process in Se–S glassy system

Nadeem Musahwar · Wasi Khan · M. Husain · M. Zulfequar · M. A. Majeed Khan

Received: 30 July 2011 / Accepted: 4 October 2011 / Published online: 30 October 2011

Abstract In the present study samples of $Se_{100-x}S_x$ has been prepared by conventional melt-quenching technique in the composition range $5 \leq x \leq 20$ (at.%). The crystallization process in glassy system was investigated under non-isothermal condition using differential scanning calorimetry (DSC) at 5, 10, 15, and 20 °C/min heating rates (ϕ). The DSC traces have been analyzed in terms of activation energy (ΔE_c) and Avrami exponent (n) using different models viz. the Starink, Flynn–Wall–Ozawa, the Friedman–Ozawa, Kissinger–Akahira–Sunose equations. The composition dependence on the glass transition temperature (T_g), the crystallization temperature (T_c), and the peak temperatures (T_p) of the samples were also determined. The analysis shows that the incorporation of sulfur content has a strong influence on the crystallization mechanism for the Se–S glassy system.

Keywords Glassy alloy · Glass transition temperature · Crystallization kinetics · DSC · Non-isothermal

N. Musahwar · M. Husain · M. Zulfequar
Department of Physics, Jamia Millia Islamia, New Delhi 110 025, India

W. Khan
Department of Applied Physics, Centre of Excellence in Materials Science (Nanomaterials), Aligarh Muslim University, Aligarh, Uttar Pradesh 202 002, India

M. A. Majeed Khan (✉)
King Abdullah Institute for Nanotechnology, King Saud University, Riyadh 114 51, Saudi Arabia
e-mail: majeed_phys@rediffmail.com

Introduction

The thermal behavior of the amorphous alloys plays an important role in determining the transport mechanism, thermal stability, and practical applications. For chalcogenide glasses, crystallization studies are of crucial importance because of some of technical applications of these materials, namely optical recording media and memory switching devices. The differential scanning calorimeter technique have so far been employed to study the crystallization process in amorphous alloys and proved to be the most effective method for such characterizing studies [1]. Recently, in thermal analysis studies several temperature control modes are used, a diversification has been considered as an aspect of the development in thermal analysis [2, 3]. The most commonly used modes are either isothermal or heating at constant rate. The drawback of the later is that the analysis of non-isothermal experiments is generally more complicated than isothermal one [1, 4]. However, in isothermal experiments it is impossible to reach a test temperature instantaneously [5].

The study of crystallization kinetics in amorphous materials by differential scanning calorimetry (DSC) methods has been widely discussed in the literature [6–8]. There is a large variety of theoretical models and theoretical functions proposed to explain the crystallization kinetics. The application of each of them depends on the type of amorphous material studied and how it was made. For glassy materials obtained in bulk form, which is the case of the alloy $Se_{100-x}S_x$ submitted to continuous heating experiments, the reaction rate of the process can be expressed as the product of two separable functions of absolute temperature and the fraction crystallized, thus satisfactory kinetic parameters: activation energy, E and reaction order, n, for describing the crystallization

reactions can be obtained. Despite some reported thermal studies for the binary Se–S system [9–11], the present contribution aims at studying the crystallization kinetics in Se–S system using different preparation method, compositions, and non-isothermal analysis methods in detail. The influence of sulfur ratio on the crystallization kinetics is reported.

Experimental

The melt-quenching technique was adopted to prepare bulk $Se_{100-x}S_x$ glasses in the composition range $5 \leq x \leq 20$ (at.%). Appropriate amounts of high pure elements were sealed in evacuated quartz ampoules under a vacuum of 10^{-4} Torr. The sealed ampoules were kept inside a furnace, where the temperature was increased up to 700 °C at the heating rate of 2–3 °C/min. The ampoules were heated at this for 10 h; during the melt process these ampoules were agitated frequently to intermix the constituents and to insure the homogenization of the melt. Quenching was done in ice cold water. Amorphous nature of these glasses was confirmed by X-ray diffraction technique (not shown here). A differential scanning calorimeter (DSC, Rheometric Scientific) was employed for the thermal behavior study. Non-isothermal runs were carried out for chosen heating rates, $\phi = 5$, 10, 15, and 20 °C/min. The temperature and enthalpy calibrations of the instrument were performed using the well known melting temperature and melting enthalpy of high purity indium supplied with the instrument. The as-quenched glasses were ground and typically 10 mg of powdered glasses was placed in a platinum pan before loading into the calorimeter.

Results and discussion

To investigate the thermal behavior of the $Se_{100-x}S_x$ system, DSC measurements were carried out at heating rates (ϕ) of 5, 10, 15, and 20 °C/min. The DSC traces for all studied compositions scanned at heating rate of 10 °C/min along with the results of $Se_{95}S_5$ are shown in Fig. 1a. All glasses exhibit endothermic slope change because of the glass transition followed by exothermic crystallization peak. The observed glass transition temperatures (T_g), the onset crystallization temperatures (T_c), and the peak temperatures (T_p) are given in Table 1 (for $\phi = 10$ °C/min).

Figure 1b displays that the three characteristic temperatures for composition $Se_{95}S_5$ are shifted to higher values with increase in heating rate. This trend indicates that the glass transition and the crystallization process behave in markedly kinetic nature. The shape of glass transition zone

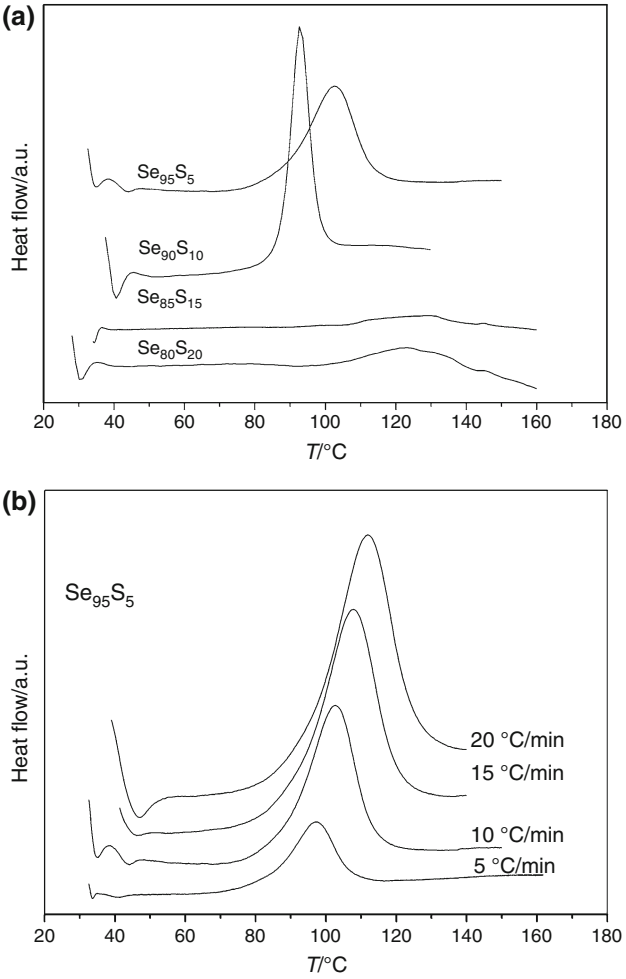

Fig. 1 **a** DSC traces for all compositions at a heating rate of 10 °C/min. **b** A typical DSC of the $Se_{95}S_5$ glass at different heating rates

becomes broader with increasing heating rate of the DSC scan. Hence, it is difficult to identify T_g for fast heating rate i.e., for 20 °C/min. As for the composition dependence of T_g, it is found that all the samples exhibited comparable glass transition temperature. In Fig. 2, the variation of T_g as a function of sulfur content is plotted for $\phi = 15$ °C/min. The supercooled region of an amorphous alloy $\Delta T = T_c - T_g$ is the widely used criteria to characterize the thermal stability of such materials. For all of the studied samples there is no significant effect of heating rate on the calculated values of ΔT. The composition dependence of ΔT is shown in Fig. 2, where the presented results are the average values for all scanned heating rates. It can be noticed that alloys with high sulfur contents ($Se_{85}S_{15}$ and $Se_{80}S_{20}$ alloy) exhibit the best thermal stability, while the other compositions show comparable values. The maximum value of ΔT for air-quenched Se–S glasses [9] was ~44 °C for alloy with $x = 6.25\%$ and 55 °C was reported for ternary system Se–S–Sn [12].

Table 1 Characteristic temperature of the $Se_{100-x}S_x$ glasses

Composition	T_g/°C	T_c/°C	T_p/°C
$Se_{95}S_5$	39	87	103
$Se_{90}S_{10}$	46	89	93
$Se_{85}S_{15}$	37	106	130
$Se_{80}S_{20}$	36	100	123

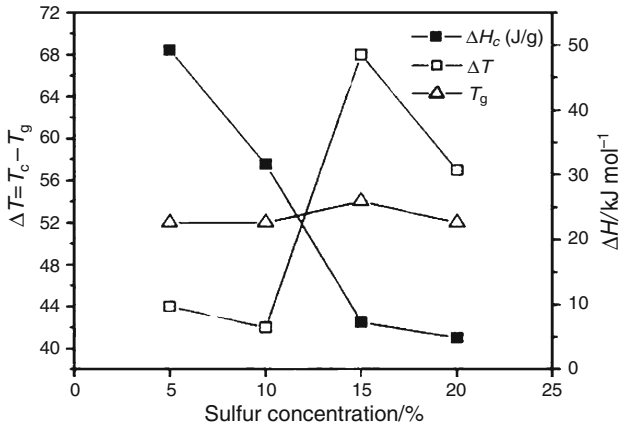

Fig. 2 Compositional dependence of glass transition temperature (T_g), thermal stability (ΔT), and crystallization enthalpy (ΔH_c)

In non-isothermal kinetics analysis, the results obtained from the thermogram are represented in terms of the crystallized volume fraction (α) as a function of temperature using

$$\alpha(T) = \frac{\int_{T_o}^{T} (dH_T/dT - dH_o/dT)dT}{\Delta H_c} \quad (1)$$

where T_o is the onset crystallization temperature, dH_T is the enthalpy of crystallization released between T and T_o, dH_o is the enthalpy of the base line of the exothermic peak and ΔH_c is the total crystallization enthalpy. In Fig. 3, the behavior of the fraction transformed (α) for a chosen heating rate ($\phi = 10$ °C/min) is represented in time scale, where $T = T - \phi t$. From the results represented in Fig. 3, it is found that 90% of solid–solid transition is completed at $\Delta t = 2.9$, 1.6, 5.3, and 3.2 min for alloys with $x = 5$, 10, 15, and 20, respectively. Hence, the alloys with highest ΔT exhibit fast solid–solid transition.

In Fig. 2, the composition dependence of the crystallization enthalpy ΔH_c is shown. Apparently, ΔH_c decreases with increase in sulfur content linearly and the alloys with low thermal satiability, ΔT exhibit the larger ΔH_c. Since the release of energy ΔH_c is associated with the metastability of the glasses [13, 14], with the exception of $Se_{80}S_{20}$, large value of ΔH_c is associated with the least stable glasses.

For the determination of crystallization activation energy, ΔE_c, from non-isothermal experiments two types of kinetic analysis methods are widely applied; isoconversion and peak methods. In an investigation study of the accuracy of known isoconversion methods, Starink [4] reported that the most accurate methods are Kissinger–Akahira–Sunose (KAS) [15–17] and the method developed by the authors [4, 18]. All the isoconversion methods require the determination of the temperature $T_f(\phi)$ at which a fixed fraction α of the total amount is transformed. In the KAS method, the relation between the temperature T_f and the heating rate ϕ is given by

$$\ln(\phi/T_f^2) = -\Delta E_c/RT_f + \text{const.} \quad (2)$$

where R is gas constant and ΔE_c is the crystallization effective activation energy. The method proposed earlier by Kissinger [19] is a peak method, where the final relation expressed in terms of T_p, i.e.,

$$\ln\left(\phi/T_p^2\right) = -\Delta E_c/RT_p + \text{const.} \quad (3)$$

Plotting of $\ln(\phi/T_f^2)$ versus $1/T_f$ enables calculation of ΔE_c from the linear fits to experimental data. The results for $\alpha = 0.6$ are shown in Fig. 4a. The most reliable isoconversion methods as reported by Ozawa [20] are Flynn–Wall–Ozawa (FWO) [21, 22], KAS and the Friedman–Ozawa (FO) method [22, 23]. The FWO model has been developed for non-isothermal analysis of crystallization in which the final relation was as follows:

$$\ln\phi = -1.0518(\Delta E_c/RT_f) + \text{const.} \quad (4)$$

By plotting $\ln\phi$ versus $1/T_f$, for chosen value of fraction transformed ($\alpha = 0.6$), the effective activation energy ΔE_c can finally be determined and shown in Fig. 4b. Friedman [23] proposed his method for nth order reaction in 1964. Later, Ozawa [24] found it is applicable to other solid–solid

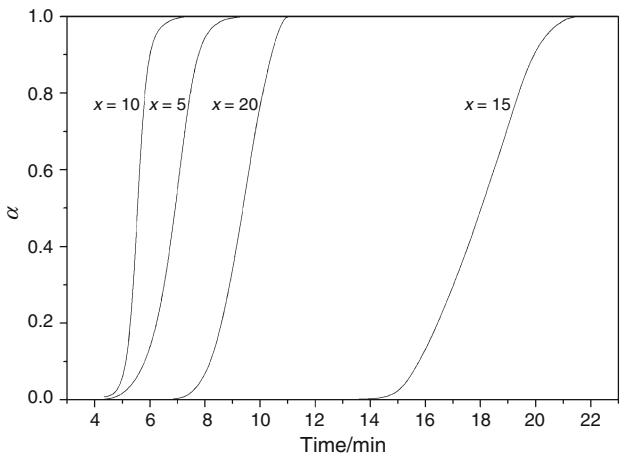

Fig. 3 Transformed fraction versus time

transition processes. According to the FO method a linear relationship of $\ln(\phi \cdot \frac{d\alpha}{dT})$ versus $\frac{1}{T}$ with slopes proportional to ΔE_c can be established from different temperature data for fixed value of fraction transformed α. The results represented in Fig. 5 shows the variation of $d\alpha/dT$ with time for $Se_{95}S_5$ alloy. The FO method gives the following relation:

$$\ln\left(\phi \cdot \frac{d\alpha}{dT}\right) = -\frac{\Delta E_c}{RT} + \text{const.} \quad (5)$$

The KAS and FWO method can be expressed in general form i.e., $\ln(\phi/T_f^s) = -A \cdot E/RT_f + \text{const.}$ In the method proposed by Starink [4, 18] $A = 1.0008$ and $s = 1.92$, i.e.,

$$\ln(\phi/T_f^{1.92}) = -1.0008\frac{\Delta E_c}{RT_f} + \text{const.} \quad (6)$$

In the present study, the activation energy ΔE_c is found to vary with α for low and high values of α (results is not shown), a result have been attributed to the high errors in the baseline interpolation for peak tails [25]. However, ΔE_c is found to be independent of α in the range 0.4–0.7. The results for chosen values of fraction transformed $\alpha = 0.4$, 0.6, and 0.7 are shown in Fig. 6 for $Se_{90}S_{10}$ (Starink method). It can be observed, the linear fitting has identical slopes for the chosen values of α. In the present study, the value of ΔE_c is calculated for $\alpha = 0.4, 0.5, 0.6$, and 0.7 for all compositions. The evaluated values of ΔE_c in Table 2 are the average values and the absolute error is the corresponding standard deviation. All the applied isoconversion methods show comparable regression of the linear least square fitting. Moreover, the results show that the KAS, Starink, and FWO methods generate consistent activation energy, ΔE_c, and consistent values of standard deviation as well. With the exception of $Se_{85}S_{15}$ alloy, the activation energies calculated using Friedman method are found to be comparable with

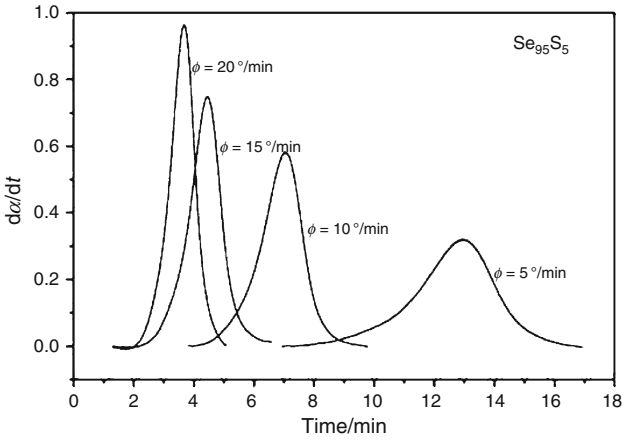

Fig. 5 Crystallization rate versus time of exothermic peaks

those obtained by other models. Here, it is worth to note that Friedman method is only recommended if transformation rates or heat evolution can be measured with high accuracy, the activation energies calculated using Eq. 5 for alloys with irregular or overlapping exothermic peaks, Fig. 1a, shows higher amplitude compared to the other applied methods.

As for the composition dependence of the activation energy, the average values of ΔE_c calculated using the equally well predicted methods; KAS, Starink, and FWO are represented in Fig. 7. For comparison, the obtained values for some of studied Se–Te alloys are 123.5 and 100 kJ/mol for $Se_{80}Te_{20}$ and $Se_{85}Te_{15}$, respectively [26, 27]. Hence, one can suggest that the effect of sulfur content increases ΔE_c compared to tellurium content. Kotkata et al. [9] found that the effect of sulfur incorporation into Se is to reduce the activation energy from 151 to 80 kJ/mol for sulfur content ranges from 4.76 to 22.22%. In agreement with the results presented in Figs. 3 and 7, it is suggested

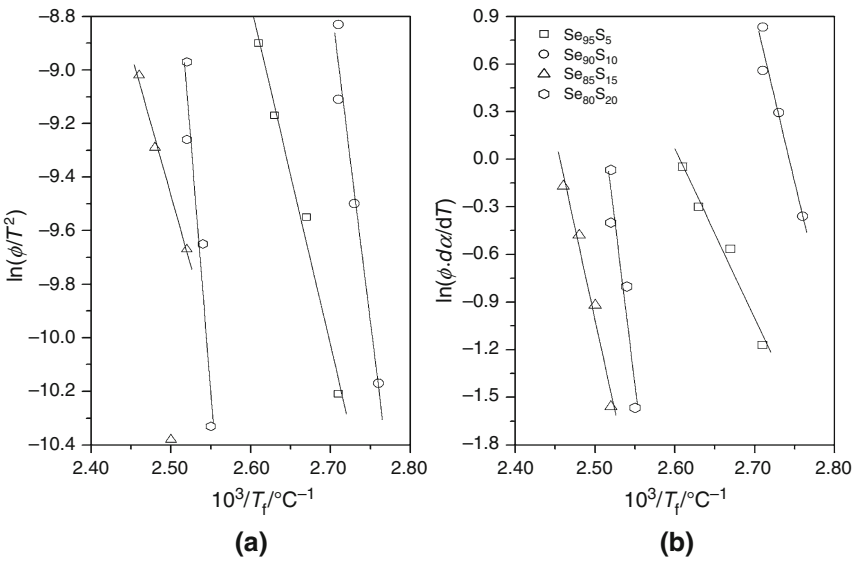

Fig. 4 Determination of activation energy using **a** KAS method, **b** FWO method

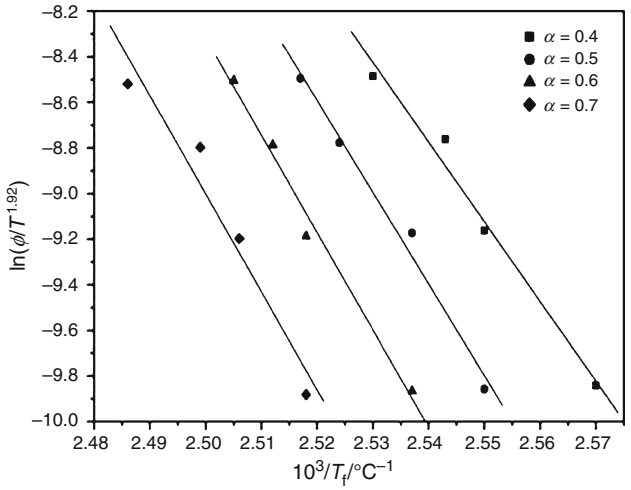

Fig. 6 Starink plot for chosen transformed fraction (α)

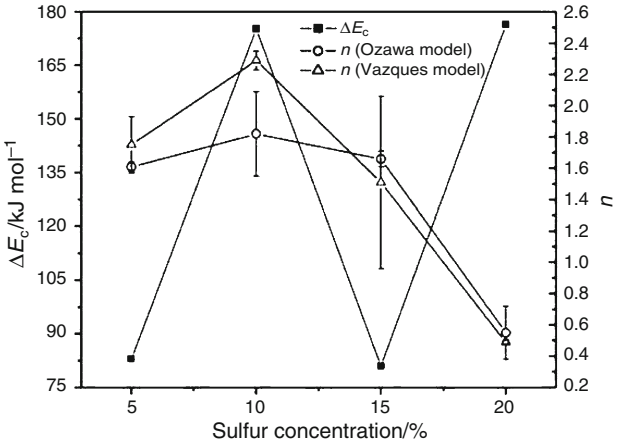

Fig. 7 Compositional dependence of activation energy and Avrami exponent

that crystallization activation energy determines the dependence of the crystallization rate on temperature, that is, the lower activation energy gives the wider temperature range of crystallization [28]. The $Se_{85}S_{15}$ alloys which shows minimum activation energy has the widest temperature range of crystallization, 42 ^{o}C, and the highest T_c as well.

For the present studied amorphous systems, we have applied two models, namely Ozawa [29, 30] and Vazquez model [31], to calculate the order of reactions occurring during linear heating. The Ozawa method is the most commonly used method in the literature, while the second is useful to monitor the heating rate dependence of n which can be observed as a deviation from linear fitting in Ozawa model. Assuming that non-isothermal crystallization process may be composed of infinitesimally small isothermal crystallization steps, Ozawa [30, 31] extended the Avrami equation to the non-isothermal case as follows:

$$\ln[-\ln(1-\alpha_T)] = \ln K(T) - n\ln\phi \tag{7}$$

where $K(T)$ is the reaction rate constant, ϕ the heating rate, and n is the Ozawa exponent which characterizes the dimensionality of the growth during the transformation. Plotting $\ln(-\ln(1-\alpha))$ versus $\ln\phi$ at given temperature, a straight line should be obtained if the Ozawa method is valid. The results based on Ozawa method are shown in Fig. 8 and the Ozawa exponents are listed in Table 2. It is worth to note that Ozawa method shows insignificant temperature dependence of n.

According to Vazquez method [31] it is possible to calculate the kinetic parameters using the following relations:

$$n = \left(\frac{d\alpha}{dt}\right)_p RT_p^2(0.37\phi E)^{-1}\ln\left(\frac{T_p^2}{\phi}\right) = \frac{E}{RT_p} - \ln q \tag{8}$$

with the exception of $Se_{85}S_{15}$ alloys, the calculated values of Avrami exponent, n, remain insensitive to the operating heating rate ϕ. The value of n in Table 2 is the average value at all heating rates for particular composition and the absolute error is the corresponding standard deviation.

The Fig. 7 shows that the calculated values of exponent n using Ozawa and Vazquez models are in good agreement, except for 10% sulphur concentration, which indicates small deviation. Moreover, both models show the same trend of composition dependence. It is worth to note that the kinetic parameters, n and ΔE_c have the same composition dependence and the calculated values of ΔE_c for alloys with sulfur content $x < 20\%$ is less than the energy of self diffusion of selenium 222 kJ/mol and the bonds

Table 2 The average values of overall kinetic parameters determined using different non-isothermal models and calculated as prescribed in the text

Composition	ΔE_c/kJ/mol				n	
	Starink	FWO	FO	KAS	Vazquez	Ozawa
$Se_{95}S_5$	101.6 ± 3.5	102.4 ± 3.3	92.1 ± 5.3	101.5 ± 3.5	1.73 ± 0.18	1.61 ± 0.03
$Se_{90}S_{10}$	175.6 ± 5.2	172.7 ± 5.0	161.7 ± 5.3	175.5 ± 5.2	2.29 ± 0.06	1.82 ± 0.27
$Se_{85}S_{15}$	94.1 ± 3.8	95.7 ± 3.6	213.1 ± 8.9	93.9 ± 3.8	1.51 ± 0.55	1.66 ± 0.05
$Se_{80}S_{20}$	336.4 ± 31.1	326.1 ± 29.6	347.7 ± 27.9	336.4 ± 31.1	0.49 ± 0.01	0.55 ± 0.17

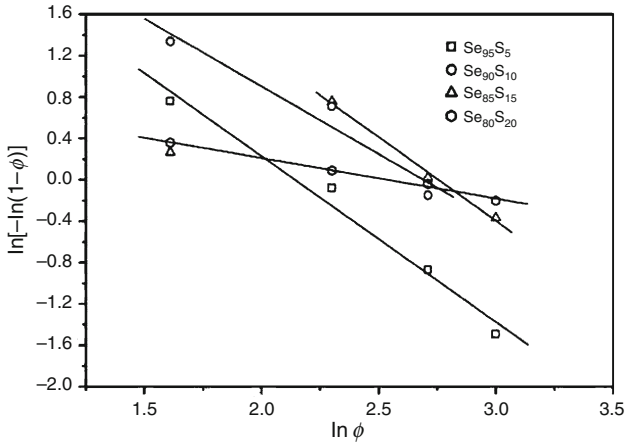

Fig. 8 Determination of Avrami exponent using Ozawa method

energies (2.48 eV for Se–Se bond and 2.13 eV for S–S bond). The activation energy for the overall reaction will generally be related to activation energy for the physical process that determines the rate of the reaction. The Avrami exponent obtained using Ozawa method cannot be related to the corresponding activation energy for $Se_{95}S_5$ and $Se_{85}S_{15}$ alloys. Hence, one can conclude that the Ozawa method is not applicable for the present studied system.

From the results represented in Fig. 7 and Table 2 it can be noted that the Avrami exponent calculated using Eq. 8 for $Se_{95}S_5$ alloy lies in the range from 1.6 to 1.9. Since the calculated ΔE_c for $Se_{95}S_5$ alloy is less than the energy of self diffusion of selenium, the possible mechanisms are diffusionless two dimensional with constant nucleation or diffusionless one dimensional growth with constant nucleation rate. For the $Se_{90}S_{10}$ and $Se_{80}S_{20}$ alloys, the diffusion mechanism can be considered, hence, the crystallization process in $Se_{90}S_{10}$ alloy is governed by diffusion-controlled two or three dimensional growth mechanism with Constant nucleation rate and it is governed by one dimensional diffusion-controlled mechanism with constant nucleation for $Se_{80}S_{20}$ alloy. Finally, the obtained Avrami exponent for $Se_{85}S_{15}$ alloy is 1.5. For $n = 1.5$, there are two possible crystallization mechanisms [32]; one is three dimensional diffusion-controlled process with constant nucleation and the other is one dimensional diffusionless process with constant nucleation rate. Recalling that the calculated activation energies for the mentioned alloy is less than the energy of self diffusion of selenium, one can rule out the possibility of diffusion-controlled mechanism. In conclusion, the sulfur content has a strong influence on the crystallization mechanism for the Se–S glassy system, alloys with low sulfur contents have two or three dimensional growth mechanism results suggests the existence of crosslinks between the selenium chains while alloys with high sulfur content have one dimensional growth mechanism which can be attributed to the accumulation of sulfur in the selenium matrix. The irregular shape and overlapping of the exothermic peaks for high sulfur content alloys support this suggestion.

Conclusions

The DSC has been used to determine the non-isothermal crystallization kinetics of the amorphous Se–S system. With the exception of Friedman method all the applied isoconversion methods give consistent values of the calculated activation energy. The Avrami exponent has been evaluated on the basis of the Ozawa and Vazquez models. The values obtained using these models cannot be related to the kinetics of amorphous-crystalline transformations. The variation in the kinetics parameters with sulfur content suggests that the addition of low sulfur content creates crosslinks between selenium chains while high amounts of sulfur results in accumulation of sulfur in the selenium matrix.

Acknowledgements The author M. A. Majeed Khan is thankful to the members of King Abdullah Institute for Nanotechnology for their kind support.

References

1. Starink MJ. The analysis of Al-based alloys by calorimetry: quantitative analysis of reactions and reaction kinetics. Int Mater Rev. 2004;49:191–226.
2. Ozawa T. Temperature control modes in thermal analysis. Pure Appl Chem. 2000;72:2083–99.
3. Ahamad MN, Vaish R, Varma KBR. Calorimetric studies on $2TeO_2$–V_2O_5 glasses. J Therm Anal Calorim. 2011;105:239–43.
4. Starink MJ. The determination of activation energy from linear heating rate experiments: a comparison of the accuracy of isoconversion methods. Thermochim Acta. 2003;404:163–76.
5. Liu L, Zhi FW, Chen L. A kinetic study of the non-isothermal crystallization of a Zr-based bulk metallic glass. Chin Phys Lett. 2002;19:1483–6.
6. Vazquez J, Barreda DGG, Lopez-Alemany PL, Villares P, Jimenez-Garay R. Crystallization of $Ge_{0.08}Sb_{0.15}Se_{0.77}$ glass studied by DSC. J Noncryst Solids. 2004;345 and 346:142–7.
7. Wang J, Liu YJ, Tang CY, Liu LB, Zhou HY, Jin ZP. Thermodynamic description of the Au–Ag–Ge ternary system. Thermochim Acta. 2011;512:240–6.
8. Surinach S, Baro MD, Clavaguera-Mora MT, Clavaguera N. Kinetic study of isothermal and continuous heating crystallization in $GeSe_2$–GeTe–Sb_2Te_3 alloy glasses. J Noncryst Solids. 1983; 58:209–17.
9. Kotkata MF, El-Fouly H, El-Behay AZ, El-Wahab LA. Transport studies of S–Se amorphous semiconductors. Mater Sci Eng. 1983;60:163–71.
10. Mahmoud EA. Crystallization kinetics of amorphous $S_{20}Se_{80}$. Therm Anal Calorim. 1990;36:1481–6.
11. Kotkata MF, Ayad FM, El-Mously MK. Photo-effect on crystallization kinetics of amorphous selenium doped with sulphur. J Noncryst Solids. 1979;33:13–22.

12. El-Shazly O, Ramadan T, El-Anany N, Mataweh HA, El-Wahidy E. Calorimetric studies of chalcogenide glasses in the system Se–S. Eur Phys J Appl Phys. 2001;13:161–5.
13. Dimitrov D, Tzocheva D, Kovacheva D. Calorimetric study of amorphous Sb–Se thin films. Thin Solids Films. 1998;323:79–84.
14. Mahadevan S, Giridhar A, Singh AK. Calorimetric measurements on As–Sb–Se glasses. J Noncryst Solids. 1986;88:11–34.
15. Kissinger HE. Reaction kinetics in differential thermal analysis. Anal Chem. 1957;29:1702–6.
16. Kujirai T, Akahira T. Effect of temperature on the deterioration of fibrous insulation materials. Sci Pap Inst Phys Chem Res. 1925;2:223–52.
17. Akahira T, Sunose T. Joint convention of four electrical institutes. Res Rep Chiba Inst Technol. 1971;16:22–31.
18. Starink MJ. A new method for the derivation of activation energies from experiments performed at constant heating rate. Thermochim Acta. 1996;288:97–104.
19. Kissinger HE. Variation of peak temperature with heating rate in differential thermal analysis. J Res Natl Bur Stand. 1956;57:217–52.
20. Ozawa T. Estimation of activation energy by isoconversion methods. Thermochim Acta. 1992;203:159–65.
21. Ozawa T. A new method of analyzing thermogravimetric data. Bull Chem Soc Jpn. 1965;38:1881–6.
22. Flynn JH, Wall LA. A quick direct method for the determination of activation energy from thermogravimetric data. J Polym Sci. 1966;B4:323–7.
23. Friedman HL. Kinetics of thermal degradation of char-forming plastics from thermogravimetry. J Polym Sci. 1964;C6:183–95.
24. Ozawa T. Applicability of Friedman plot. J Therm Anal Calorim. 1986;31:547–51.
25. Malek J, Cernoskova E, Svejka R, Sestak J, Van der Plaat G. Crystallization kinetics of $Ge_{0.3}Sb_{1.4}S_{2.7}$ glass. Thermochim Acta. 1996;280–281:353–61.
26. Afify N. Calorimetric study on the crystallization of a $Se_{0.8}Te_{0.2}$ chalcogenide glass. J Noncryst Solids. 1992;142:247–59.
27. Calventus Y, Surinach S, Baro MD. Crystallization mechanisms of a $Se_{85}Te_{15}$ glassy alloy. J Phys Condens Matter. 1996;8:927–40.
28. Suzuki T, Arai Y, Ohishi Y. Crystallization processes of Li_2O–Ga_2O_3–SiO_2–NiO system glasses. J Noncryst Solids. 2007;353:36–43.
29. Ozawa T. Kinetic analysis of derivative curves in thermal analysis. J Therm Anal Calorim. 1970;2:301–24.
30. Ozawa T. Kinetics of non-isothermal crystallization. Polymer. 1971;12:150–8.
31. Vazquez J, Wagner C, Villares P, Jimenez-Garay R. Glass transition and crystallization kinetics in $Sb_{0.18}As_{0.34}Se_{0.48}$ glassy alloy by using non-isothermal techniques. J Noncryst Solids. 1998;235–237:548–53.
32. Hsiao A, McHenry ME, Laughlin DE, Kramer MJ, Ashe C, Ohkubo T. The thermal, magnetic, and structural characterization of the crystallization kinetics of $Fe_{88}Zr_7B_4Cu_1$, an amorphous soft magnetic ribbon. IEEE Trans Magn. 2002;38:3039–44.